Electron backscatter and impedance in one-dimensional space-charge-limited diodes

N. R. Pereira
Maxwell Laboratories, Incorporated, San Diego, California 92123

(Received 29 April 1983; accepted for publication 4 August 1983)

Megavolt electrons striking a high-Z anode/bremsstrahlung X-ray converter anode are partially reflected into the anode-cathode gap of the diode. The diode charge density is higher than without reflection, and the current density is lower. A quantitative estimate for one-dimensional flow yields a reduction from Child–Langmuir by up to 25% for unipolar flow. For bipolar flow, the ion current can increase twofold.

PACS numbers: 52.75.Di, 52.90. + z

Hard x rays can be generated in a megavolt electron diode with an anode made of high-Z material such as tantalum, bismuth, or uranium. For a given material and electron energy, the x-ray output is proportional to the electron current. It is well known that in x-ray production calculations the backscattered electrons must be reused; however, the influence of backscatter on diode current is widely ignored.[1] The approximate representation of backscatter in a one-dimensional diode in the present work suggests that the diode current may decrease by 25% from the Child–Langmuir value for electrons only. For space-charge limited bipolar flow, there is a similar reduction in the electron current, but the ion current is considerably larger than without backscatter. These results are consistent with the behavior of reflex triodes.

One-dimensional diode models do apply only at a low current density or with a strong magnetic guide field. In contrast, realistic high-current x-ray diodes are essentially two dimensional and are not readily treated with analytical means. However, numerical PIC diode codes can be coupled to Monte Carlo codes to account for the backscatter. Experimentally and computationally, the effect of the anode material[2] on some diode properties, notably pinching, is indeed considerable, while, e.g., the total current is relatively unaffected.

The large Coulomb field from high-Z nuclei causes efficient bremsstrahlung production and is responsible for electron backscatter. Backscatter is due to single and multiple large angle scattering, proportional to Z^2. Energy loss of the primary electron, electron-electron interaction, is proportional to Z only. Therefore, backscatter is intrinsic to an x-ray converter.

Much of the experimental data on backscatter of single electrons is available in the literature.[3–5] The fraction of electrons backscattered from a thick target with atomic number $Z \geqslant 60$ at perpendicular incidence with incoming energy $V_0 = 1$–3 MeV is in the range 0.4–0.6. This fraction decreases at higher energies, although there is a peak in the backscatter fraction around 1 MeV, depending on material. For low-Z materials, the backscatter is negligible, less than a few percent for graphite or beryllium.

An energy distribution of the backscattered electrons is given in Fig. 1. For lead at $V_0 = 1.75$ MeV, the backscatter energy spectrum peaks at 0.83 V_0, the average energy exceeds 0.75 V_0, and about one-third of the incoming energy is reflected. The spectra for low and high-Z materials are comparable at low energy; they differ mainly in the energy of the peak and the number of electrons backscattered at the peak energy.

Other data[4] suggest that oblique incidence under angle A multiplies the backscatter by a factor $(1 + \cos A)^{-p}$, where p is $9Z^{-1/2}$. Also, the backscatter increases with target thickness below about 40% of the electron range; any target thickness over half the electron range makes a thick target.

No satisfactory analytical treatment for backscattering from a discontinuous boundary[6–9] seems to exist. Most calculations employ Monte Carlo methods with typically good results.[10]

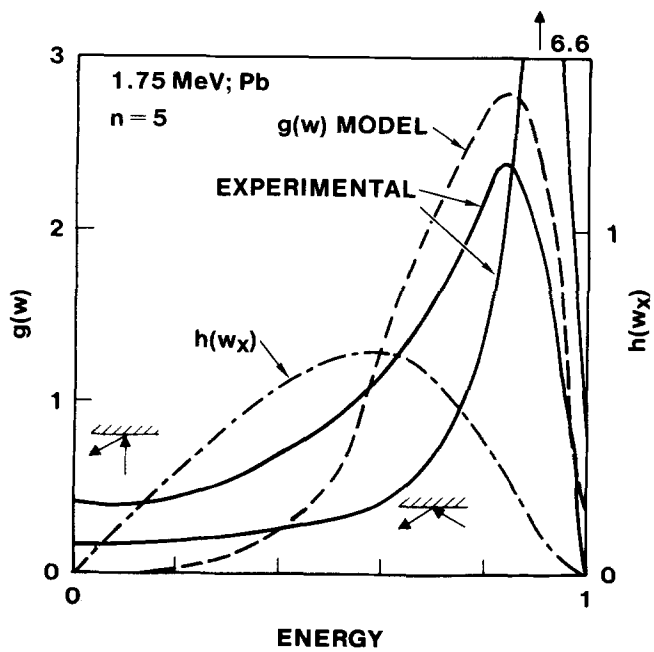

FIG. 1. Representative experimental electron backscatter energy spectra (solid lines) at 1.75-MeV energy incident on lead as shown. The dashed line is the approximate analytical spectrum $g_n(w)$ for $n = 5$. The dash-dot line is the corresponding perpendicular energy spectrum (after Franck, Ref. 3).

 0021-8979/83/116307-04$02.40

In addition to the energetic backscattered electrons, there are also slow secondary electrons below 50 eV or so. These electrons stay close to the anode surface where they will become part of the anode plasma; they are henceforth ignored. There are also energetic secondaries (delta rays) which are included under the backscattered primary electrons. The total may be called the retrofugal flux.[5]

In reflex triodes[11] used for intense ion beam generation, there is a population of trapped electrons that pass through the thin anode foil and reenter the diode on the other side. These electrons are reaccelerated in this second diode and pass through the foil again to reappear in the first diode, but with lower energy and a certain average scattering angle. Transmission through the foil repeats until the electrons have lost all their energy. Similarly, in the steady state of a diode with high-Z anode the backscattered electrons are reaccelerated and strike the anode again with their new energy and angular distribution, etc. The electrons are now trapped between the potential of the cathode and the partly reflecting anode.

An upper limit for the impedance is obtained by considering purely perpendicular reflection without energy loss from the anode. Reflected electrons now retrace their paths until they are assumed to be absorbed at the cathode. For a given current density of the forword going electrons, the charge density in the diode is now twice the charge density without reflecting electrons. Alternatively, the forward current density with specularly reflecting electrons is half the Child–Langmuir value.

With an arbitrary energy spectrum for the backscattered electrons in the reflex diode, in the one-dimensional nonrelativistic approximation, the analysis is standard. There are two cases: pure electron flow, and opposing electron and ion flow (bipolar flow).

For a large gap spacing the current density can be low enough to avoid the ion current from the anode. With only electrons and no ions, the diode contains space charge from both the primary and the reflecting electrons. The electron density is

$$n_e = \frac{j_e}{e}\left[1/v_e(x) + 2\sum_i R_i \int h_i(W_x)/v_b(x)dW_x\right],$$

where j_e is the electron current density, $-e$ the electron charge, and v_e the velocity of the electrons coming from the cathode. Also, R_i is the fraction of the primary current that is backscattered in the ith reflection, $h_i(W_x)$ the energy spectrum of W_x, the initial backscattered kinetic energy component perpendicular to the electrodes and parallel to the guide magnetic field, and v_b the velocity of the backscattered electrons. The factor 2 accounts for the backscattered electrons returning to the anode. The integration over parallel energy W_x is cut off at the turning point where v_b vanishes.

At this stage, the spectrum $h(W_x)$ can be approximated by some assumed functional form, e.g., a delta function or a constant. Then the analysis becomes identical to that of the reflex triode.[12] Assuming that backscatter of half the electrons corresponds to roughly one full transit through the anode in the reflex triode suggests that the impedance may increase by a factor 2 (see Fig. 2 in Ref. 12).

Poisson's equation, using nonrelativistic expressions for the velocity, becomes in normalized form

$$\frac{d^2s}{dx^2} = \frac{4}{9}\frac{j_e}{j_0}\left[s^{-1/2} + 2\sum R_i \int_{1-s}^{1} \times dw_x\, h_i(w_x)(s-1+w_x)^{-1/2}\right],$$

where x is the distance from the cathode normalized to the gap spacing d, $s = s(x)$ the electrostatic potential normalized to the anode potential V_0, and $w_x = W_x/eV_0$ the normalized kinetic energy in the x direction perpendicular to the electrodes. The current density is j_e, and j_0 is the nonrelativistic Child–Langmuir current density that applies when the reflected fraction R_i vanishes.

Multiplication with ds/dx (assumed positive) and using the boundary condition $ds/dx = 0$ at the cathode appropriate for space-charge limited flow gives

$$\left(\frac{ds}{dx}\right)^2 = \frac{j_e}{j_0}G(s),$$

where

$$G(s) = \frac{16}{9}[s^{1/2} + F(s)],$$

and

$$F(s) = 2\sum_i R_i \int_{1-s}^{1} dw_x\, h_i(w_x)[w_x - (1-s)]^{1/2}.$$

Further integration across the gap of ds/dx gives the current density j_e as

$$j_e/j_0 = I^2,$$

where

$$I = \int_0^1 ds\, G^{-1/2}(s).$$

The backscattered electron energy distribution $h_i(w_x)$ and the reflection coefficient R_i determine I but, in general, the dependence is not expressible in analytic form and must be found numerically. A simple case is to assume a delta function distribution that mocks up constant perpendicular energy loss Δw_x in each bounce:

$$h_i(w_x) = \delta(w_x - 1 + i\Delta w_x),$$

where H is the Heaviside function.

For a high-Z anode a reasonable estimate for Δw_x is of order $\Delta w_x \simeq 0.25$, and $R_i = 0.6$. Numerical computation shows that in this case the current density is 65% of the Child–Langmuir value.

For a better estimate the functional form $h(w_x)$ must be calculated more precisely. Nonrelativistically, w_x is given by the total kinetic energy K and backscatter angle θ:

$$W = K\cos^2\theta.$$

For given incident angle and energy distribution, the angle and energy dependent backscatter[3,5] is usually in the form of a backscattered energy flux $f_i(K,\theta)$, where i indexes the incident conditions. The parallel backscatter spectrum is then

$R_i\, h_i(W_x)$

$$= 2\pi \int_0^{\pi/2} d\theta \sin\theta \int_0^{eV_0} dK f_i(K,\theta)\delta(K\cos^2\theta - W_x)$$

(eV_0 is the maximum incident energy). For the first backscatter, the electrons are monoenergetic and they come in perpendicular to the anode. The backscatter distribution for this case is known from measurements or computations so that $h_i(W_x)$ can be calculated.

For the next order $h_x(W_x)$, one needs to convolve the backscatter over the angle of incidence and the incident energy, followed by an integration over exit angle. Higher order spectra $R_i\, h_i$ can be done similarly, and in the absence of experimental data one could calculate the backscatter from a computer code.

For perpendicular incidence, the angular distribution over the relevant range (about the normal) follows to a good approximation the cosine of the exit angle, weakly dependent on exit energy.[3] For oblique incidence and high-Z materials, the energy distribution becomes strongly peaked about the direction of elastic scattering at higher energy, but at lower energy the angle of incidence is unimportant. However, the perpendicular energy at oblique exit angles is reduced compared to perpendicular exit and it is reasonable to neglect effects on the energy spectrum due to angle of incidence. We will use the convenient approximation

$$f_i(K,\theta) = g(K)\cos\theta,$$

with $g(K)$ a universal energy spectrum valid for all angles of incidence.

Theory does not seem to give simple functional form for the energy spectrum that agrees with experiment. Our Monte Carlo computations at a low backscatter energy suggest a power law, $g(K) = K^n$, with exponent n about three, while the spectrum should also decrease rapidly near the incident energy. Ignoring the finite backscatter[5] at the incident energy, we take as the model spectrum

$$g(K) = A_n\, w^n(1-w),$$

where $w = K/eV_0$ and A_n is a normalization constant determined by the experimentally observed backscatter fraction

$$R = J_{\text{back}}/J_{in} = 2\pi \int_0^{\pi/2} d\theta \sin\theta\cos\theta \int_0^1 dw\ g(w),$$

or

$$A_n = R\,(n+1)(n+2)/\pi.$$

The power $n = n(Z)$ can be chosen such that the maximum of g, at $w_x = n/(n+1)$, coincides with the maximum of the experimental spectrum. Our g underestimates the unimportant low-energy tail.

From the approximate energy spectrum $g(K)$, the parallel energy spectrum becomes, using $m = \cos^2\theta$ and $w_x = K_x/eV_0$

$$Rh(w_x) = A_n \int_{w_x}^1 dm\, w_x^n(1 - w_x/m)/m^{n+1},$$

the lower bound on the integration being due to integration over the delta function. Further integration and use of the normalization gives

$$h(w_x) = (n+2)/n\pi\{1 - w_x^n[1 + n(1-w_x)]\}.$$

The energy spectrum $g(w)$ and the parallel energy spectrum $h(w_x)$ are plotted in Fig. 1 together with experimental data.[3] The peak in the parallel energy spectrum is shifted toward lower energy as expected from the cosine squared factor in the energy. The best choice for n appears to be in the range $n = 4$–6; the results should be insensitive to n.

The summation over reflections in $F(s)$ gives a factor $R/(1-R)$, and also the integration over w_x can be performed explicitly; however, the final integal over G must be done numerically. Figure 2 shows the result of this computation. The form of the distribution, parametrized by n, is indeed relatively unimportant. For a tantalum anode at 1 MeV, we estimate $n = 4$ and $R = 0.6$, suggesting a reduction in current density from Child–Langmuir to 80%.

The change in current density for small reflection coefficient R can be calculated analytically. At $R = 0$,

$$d(j_e/j_0)/dR = 2I\, dI/dR = 2dI/dR\,|_{R=0},$$

where

$$dI/dR\,|_{R=0} = -3/4 \int_0^1 ds\, s^{-3/4} \times \int_{1-s}^1 dw_x\, h(w_x)[w_x - (1-s)]^{1/2}.$$

The perpendicular energy spectrum $h(w_x)$ can be approximated by (see Fig. 1),

$$h(w_x) = a\, w_x(1 - w_x),$$

where $a = 2.6$. Then

$$\int_{1-s}^1 dw_x\, h(w_x)[w_x - (1-s)]^{1/2} = 4as^{5/2}(7 - 4s)/105,$$

and

$$dI/dR = 244a/5775 = 0.11.$$

This value, the dashed line in Fig. 2, is in good agreement with the computed slope at $R = 0$.

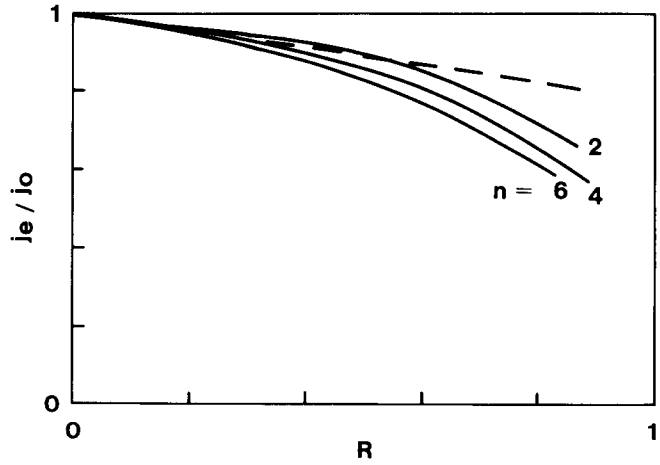

FIG. 2. Current density in a one-dimensional backscatter diode with backscatter electron spectrum $g_n = A_n\, w^n(1-w)$ normalized to the one-dimensional single specie Child–Langmuir current density j_0. The dashed line is the analytical estimate for the current change with backscatter fraction R at $R = 0$.

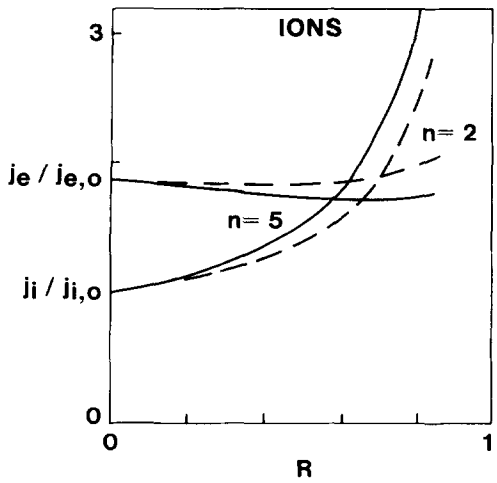

FIG. 3. Electron current density j_e and ion current density j_i in bipolar flow for electron backscatter spectra with parameter $n = 2$ and 5 as function of the backscatter fraction R. The normalization for j_e is the one-dimensional single specie Child–Langmuir electron current density $j_{0,e}$, which the normalization for j_i is the on current density $j_{i,0}$ in one-dimensional Child–Langmuir flow with electrons and ions.

When the electron current density is sufficiently large, ions can be extracted from the anode. The ions flow toward the cathode, and the diode space charge is supplemented by the ionic charge. The integrand $G(s)$ becomes in this case of bipolar flow[12–14]

$$G(s) = \frac{16}{9}\{s^{1/2} - \alpha[1 - (1-s)^{1/2}] + F(s)\},$$

where $\alpha = j_i/j_e(m_i/m_e)^{1/2}$ is the normalized ion current. For the simplest case, space-charge limited flow at the anode, $\alpha = 1 + F(1)$.

Figure 3 presents the electron current density including backscatter and ions. For $R = 0$ Langmuir's value $I = 1.86$ is recovered; for nonzero backscatter the electron current changes little, less than 8% for a backscatter spectrum with $n = 5$ and even less for $n = 2$. However, the ion current increases by a much larger factor of order 1.8 at $R = 0.6$. Similar observations apply in ion diodes (e.g., Fig. 2 in Ref. 12).

Relativistic effects can be studied in an analogous manner by using the appropriate relations for the electron velocity, and its integral with respect to energy. This is not done here, because relativity does not introduce qualitative changes in Child–Langmuir flow, and only a minor effect is expected. The major approximations are the backscatter model, and especially two-dimensional effects; these are usually treated with large codes.[2]

It is tempting to speculate on observable consequences of electron backscatter besides the impedance reduction found here, and the broadening of an electron pinch discussed in Ref. 2. In most common diodes, however, backscatter effects tend to be swamped by other physics, e.g., neutral plasma blowoff and subsequent diode current increase. The factor 2 enhancement in the ion current expected from backscatter in such a diode is easily masked by a small charge in the much larger electron current. Changes in dominant electron currents are more easily observed, especially if electrons can be scattered outside the diode toward conductors that do not normally carry current, and this may have been observed in some experiments.[15]

ACKNOWLEDGMENTS

Discussions with J. Shannon, J. Rauch, and N. Rostoker stimulated this work, which was supported by the Defense Nuclear Agency.

[1]Except in unpublished work by S. A. Goldstein, P. F. Ottinger, R. J. Barker, and R. A. Meger, JAYCOR report TDP 200-80-008-FR (1980).
[2]D. J. Johnson and S. A. Goldstein, J. Appl. Phys. **48**, 2280 (1977), J. P. Quintenz and M. M. Widner, J. Appl. Phys. **51**, 4688 (1980).
[3]W. Bothe, Z. Naturf, Teil. A **4**, 542 (1949); H. Frank, Z. Naturf. Teil. A **14**, 247 (1959); K. A. Wright and J. S. Trump, J. Appl. Phys. **33**, 687 (1962).
[4]H. Niedrig, J. Appl. Phys. **53**, R15 (1982), is a recent summary of backscatter below 100 keV.
[5]R. W. Dressel, Phys. Rev. **144**, 332 (1966); Phys. Rev. **144**, 344 (1966).
[6]R. D. Birkhoff, in *Handbuch der Physik*, Vol. XXXIV, edited by S. Flügge (Springer, Berlin, 1958).
[7]L. V. Spencer, Phys. Rev. **98**, 1597 (1955).
[8]R. F. Dashen, Phys. Rev. A **134**, 1025 (1964).
[9]J. H. Jacob, J. Appl. Phys. **45**, 467 (1974).
[10]C. D. Zerby and F. L. Keller, Nucl. Sci. Eng. **27**, 190 (1967).
[11]S. Humphries, Jr., J. J. Lee, and R. N. Sudan, J. Appl. Phys. **46**, 187 (1975).
[12]J. M. Creedon, I. D. Smith, and D. S. Prono, Phys. Rev. Lett. **35**, 91 (1975); also, D. S. Prono, J. M. Creedon, I. Smith, and N. Bergstrom, J. Appl. Phys. **46**, 3310 (1975).
[13]T. M. Antonsen and E. Ott, Phys. Fluids **19**, 52 (1976); Appl. Phys. Lett. **28**, 424 (1976); J. W. Poukey, Appl. Phys. Lett. **26**, 145 (1975).
[14]For a summary see, R. B. Miller, *Intense Charged Particle Beams* (Plenum, New York, 1982); or V. M. Bystritskii and A. N. Didenko, Usp. Fiz. Nauk **132**, 91 (1980) [Sov. Phys. Usp. **23**, 576 (1981)].
[15]T. Lockner (private communication).